Phase Identification and Temperature-Dependent Magnetization of Ti-Rich Titanomagnetite ($0.5 \leq x \leq 1$) in Different Atmospheres

S. Lan[1], C. Groschner[1], J. Runco[1], A. Wise[1], M. Díaz-Michelena[2], D. Laughlin[1], and M. E. McHenry[1]

[1]Materials Science and Engineering, Carnegie Mellon University, Pittsburgh, PA 15213 USA
[2]Payloads Technologies and Space Sciences Department, Instituto Nacional de Técnica Aeroespacial(INTA), Madrid, Spain

Reduced titanomagnetite solid solutions, $x\mathrm{Fe_2TiO_4} - (1-x)\mathrm{Fe_3O_4}$, with $0.5 \leq x \leq 1$, were synthesized by sintering in 99.996% pure flowing argon. Samples showed a systematic variation in the second phase amount as a function of x. A wustite second phase primarily forms near the surface of titanomagnetite pellets. The amount of wustite decreases with increasing Ti concentration. XRD data confirms that samples with $x > 0.8$ have less than 1% wustite. M(T) curves were measured by vibrating sample magnetometer (VSM). A magnetization hump is observed in M(T) during heating and explained by ferrimagnetic phases formed by exsolution and precipitation processes. These phases were identified as titanomaghemite and magnetite by fitting M(T) cooling curves with a multi-phase Brillouin function.

Index Terms—**Martian mineral, remnant magnetization, thermal magnetic property, titanomagnetite.**

I. INTRODUCTION

TITANOMAGNETITE (TMs), $x\mathrm{Fe_2TiO_4}$-$(1-x)\mathrm{Fe_3O_4}$, are magnetic minerals whose remnant state may contribute to planetary field anomalies. Ti-rich TMs ($0.5 \leq x \leq 1$) have magnetic transitions in the day to night temperature swing on Mars [1]. Titanomagnetite is a solid solution of magnetite and ulvospinel with a spinel structure and cubic close packed oxygen anions, represented as a pseudo-binary line in Fe-Ti-O ternary phase diagram [2]. Synthesis of $\mathrm{Fe_{3-x}Ti_xO_4}$ requires control of oxygen fugacity. It is possible to get different phases in synthesized TM depending on the atmosphere. Given the composition of the Martian lower atmosphere (0.13% of O_2) [3], titanomagnetites may exist in a more reduced state. Reduced titanomagnetites have been studied in iron-making process [4] and to refine rare earth metal from ore [5]. Here we report the temperature-dependent magnetization of reduced titanomagnetites ($0.5 \leq x \leq 1$) which can give insight into the magnetic transition of minerals on Mars. The magnetic phases identified during heating and cooling can help to catalog contributors to the crustal field of Mars [6], [7].

II. EXPERIMENTAL PROCEDURE

Reduced titanomagnetite (TM) with different weight % of wustite were synthesized by sintering in 99.996% pure argon. Solid solutions were prepared in two steps. The first step consisted of synthesis of $\mathrm{Fe_2TiO_4}$ by sintering $\mathrm{TiO_2}$, $\mathrm{Fe_2O_3}$ and extra Fe [1]. Extra Fe was added to prevent Fe-deficiency in the synthesized ulvospinel. The powder mixtures were ball milled for 10 min and then wet ground with acetone in mortar. After drying, the mixtures were pressed into pellets and put into tube furnace flushed with Ar. Dwell times of 72 hours in the furnace at 1150°C were used and the pellets were then cooled to

room temperature in the argon atmosphere. Powder diffraction showed the obtained ulvospinel was single phase:

$$2\mathrm{Fe_2O_3} + 3\mathrm{TiO_2} + 2\mathrm{Fe} = 3\mathrm{Fe_2TiO_4}. \tag{1}$$
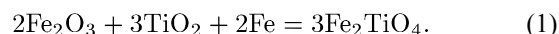
$\mathrm{Fe_2TiO_4}$ and $\mathrm{Fe_3O_4}$ mixtures were sintered at 1100°C. $\mathrm{Fe_3O_4}$ was bought from Alfa Aesar®. After sintering 72 h, the temperature was decreased to 750°C and samples were then quenched in ice water. The desired TM composition was produced by varying the atomic % of $\mathrm{Fe_2TiO_4}$ in $\mathrm{Fe_3O_4}$. TM samples with $x = 0.5, 0.6, 0.7, 0.8, 0.9$ and 1.0, respectively, are designated TM50–100:

$$(1-x)\mathrm{Fe_3O_4} + x\mathrm{Fe_2TiO_4} = \mathrm{Fe_{3-x}Ti_xO_4}. \tag{2}$$
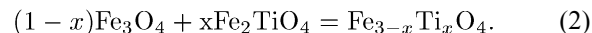
As-quenched TM50–TM100 samples were prepared as 5 mm thick pellets with a 19.2 mm diameter. The TM60 pellet surface was scanned by a Philips XL30 Scanning Electron Microscopy (SEM). A TM50 pellet was polished layer by layer from the gas-solid surface side and each layer was characterized by a Panalytical X'Pert X-ray Diffraction (XRD). Cu $\mathrm{K_{\alpha 1}}$ (1.5406 Å) and Cu $\mathrm{K_{\alpha 2}}$ (1.5444 Å) radiation was used. TM50–TM100 pellets were crushed into powder. Normal ($15 \leq 2\theta \leq 90$) and high angle ($82 \leq 2\theta \leq 143.25$) scans were performed on powders. Temperature dependent magnetization was measured using a Lake Shore 7404 VSM with a furnace attachment. Ar was flushed into the furnace to reduce atmospheric oxygen. The temperature was increased from 30°C to 700°C and then decreased to 30°C at 5°C per minute. The applied field during heating and cooling is 0.3 T. TM70 and TM90 after VSM were characterized by 10-h slow XRD scans.

III. RESULTS

Wustite peaks are present in TM50–80, as shown in Fig. 1(a). The weight % of wustite is identified by direct comparison method [8]. Fig. 1(b) shows wt.% of wustite second phase versus at.% of ulvospinel (x). The wustite in TM50, TM60, TM70 and TM80 are 18.5 wt.%, 11.53 wt.%, 6.24 wt.% and 0.95 wt.%, respectively, i.e., the amount of wustite decreases as the x increases. For $x > 0.8$ almost single phase solid solution formed; while for $x < 0.6$, more than 12% of wustite is present
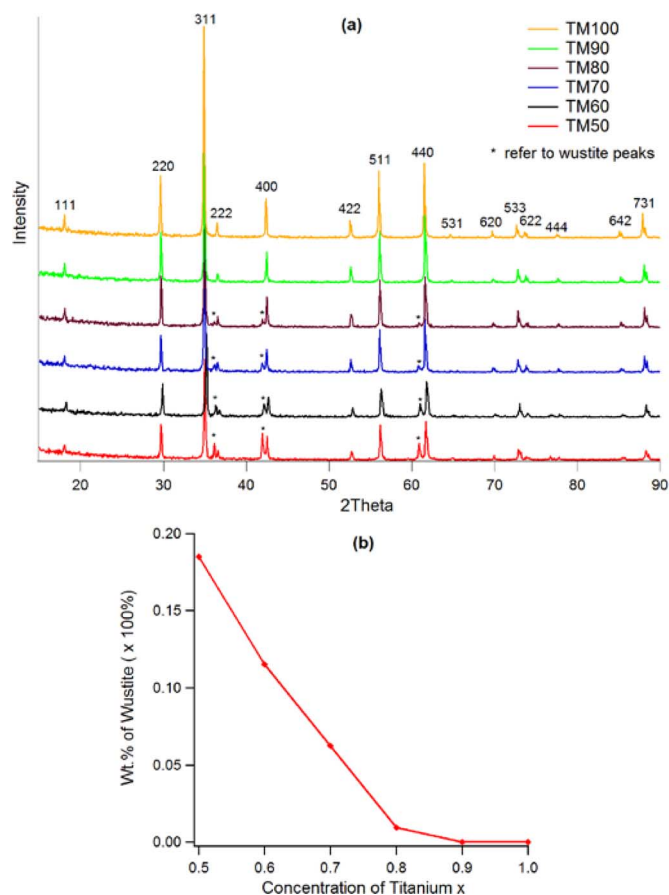
Fig. 1. (a) X-ray diffraction result for TM50 to TM100. Peaks indicated by * correspond to the wustite peaks (111), (200) and (220), respectively. (b) Amount of wustite secondary phase versus titanomagnetite nominal composition.
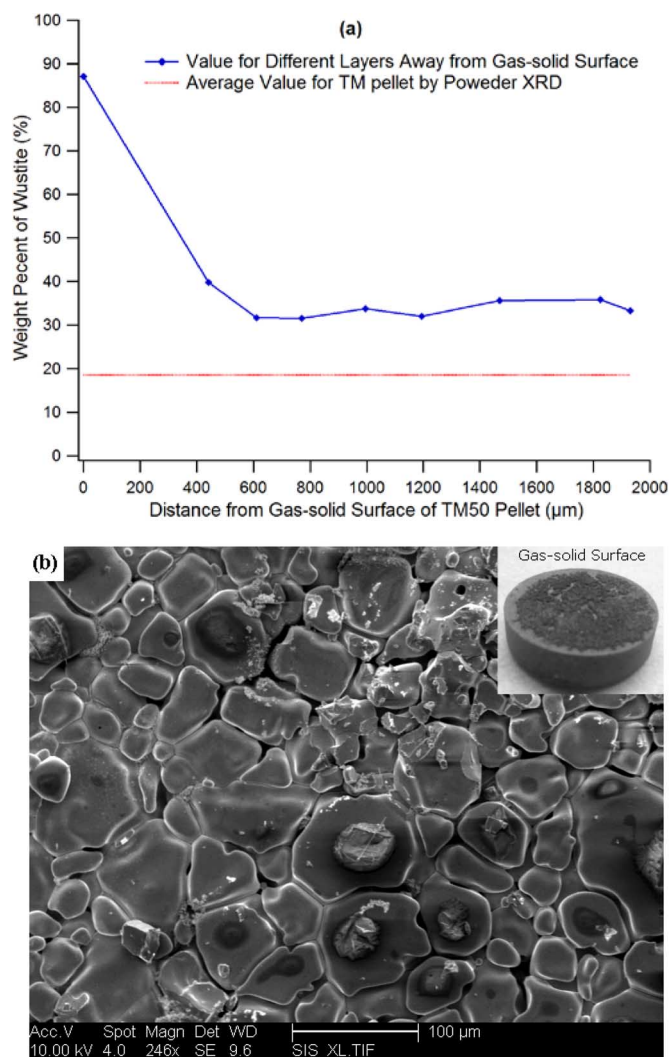
Fig. 2. (a) Wt.% of wustite in different layers in TM50 Pellet. (b) SEM image of the surface of a TM60 pellet. Inset: a picture of TM50 pellet: top face is gas-solid; bottom face is solid-solid surface.

under the sintering conditions in this study. Sample will deviate from nominal composition because of wustite formation. The compositions can be corrected by eliminating effect of wusite, as shown in Table I. The amount of wustite secondary phase in different layers of a TM50 pellet is indicated in Fig. 2(a). The gas-solid surface has 87.04% wustite and the wt.% decreases as the distance from the gas-solid surface increases to 600 μm. After that, the amount of wustite fluctuates around 33.37%. The average wustite amount in the TM50 pellet was 18.5% with the solid-solid surface side having a wt.% of wustite much less than 18.5%. Fig. 2(b) shows an SEM image of surface of TM60 pellet. Sintered pellets are porous, increasing the reaction surface. The average grain size is ~35 μm.

Lattice parameters for as-quenched TM samples are calculated from high angle XRD by Cohen's method [9]. Fig. 3 shows TM50 to TM100 results. A calculated Fe_3O_4 (Mag) lattice parameter is 8.386 Å, smaller than 8.396 Å (JCPDS-19-0629) but larger than maghemite (Magh) 8.3515 Å (JPCDS-39-1346). The calculated Fe_2TiO_4 (Ulvo) is 8.5353 Å, the same as 8.5352 Å (JCPDS-34-0177). In Fig. 3, three straight lines plot the lattice constant for pseudo-binary solid solutions according to Vegard's law.

Lattice parameters for TM70 and TM90 after VSM are also included. A master curve [10] in Fig. 4(b) shows an increasing

TABLE I
CORRECTED COMPOSITION FOR TM SAMPLES WITH WUSTITE SECOND PHASE

$Fe_{3-x}Ti_xO_4$	TM50	TM60	TM70	TM80
Nominal x	0.5	0.6	0.7	0.8
Corrected x	0.619	0.682	0.749	0.808

Fe^{2+}/Fe^{3+} ratio as the unit cell parameter increases. Based on the master curve and lattice parameters, the Fe^{2+}/Fe^{3+} ratio for TM samples is illustrated in Fig. 4(a).

Fig. 5 shows magnetization versus temperature for powder samples during heating (a) and cooling (b). Fig. 5(a) shows a magnetization hump beginning around 300°C and ending at 580°C. A systematic decrease of magnetization as increasing mol.% of Fe_2TiO_4 is observed below 300°C. The magnetization drops above 580°C. Fig. 5(b) shows magnetization increases with decreasing temperature. There are prominent changes in
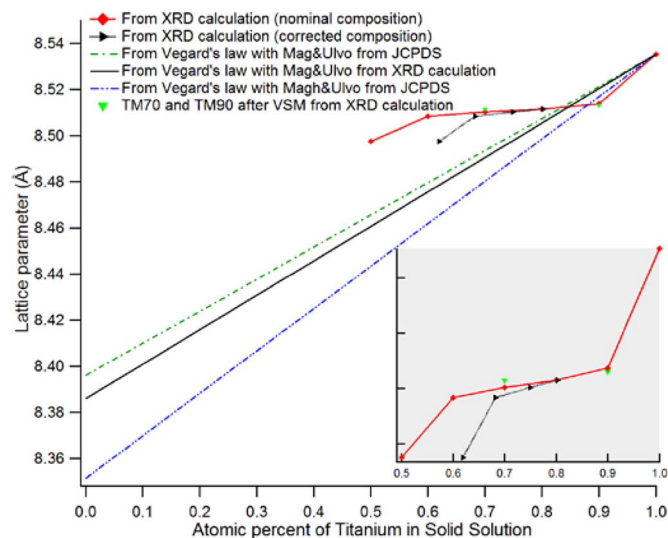
Fig. 3. Lattice parameters from XRD calculation and from Vegard's law. Inset: lattice parameter for as-quenched TM samples and TM70, TM 90 after VSM.

the slope of M(T) in temperature ranges denoted I, II, and III, indicating magnetic phase transitions.

IV. DISCUSSION

A. Redox States for TM Samples

Based on lattice parameters, synthesized ulvospinel is single phase and commercial magnetite has some maghemite. Without oxidization or reduction, the lattice parameter of solid solutions would lie ideally on the black line of Fig. 3. Reduced or oxidized titanomagnetites should lie between green and blue dashed lines in Fig. 3. For TM50–TM80, the presence of wustite as a second phase indicates that they are reduced to the FeO-Fe_3O_4-Fe_2TiO_4 region in Fe-Ti-O ternary phase diagram. The oxygen fugacity around the sample pellets in the sintering atmosphere was below the exact $f(O_2)$ for titanomagnetite pseudo-binary system. Since $\Delta G_{(Fe^{3+}\to Fe^{2+})}$ is smaller than $\Delta G_{(Fe^{2+}\to Fe)}$, the reduction happens in magnetite and maghemite, thus increasing Fe_2TiO_4 at.% in $Fe_{3-x}TiO_4$ solid solution. The deviation from nominal composition by reduction results in a larger lattice parameter, as indicated in Fig. 3. For TM90, partial oxidation of magnetite to maghemite is suggested by the smaller lattice parameter. Titanomaghemitization decreases the at.% of Fe_2TiO_4 and introduces vacancies. For TM100, neither oxidation nor reduction occurs.

Redox states of TM50 to TM90 are confirmed by the Fe^{2+}/Fe^{3+} ratio R in Fig. 4. The R for single phase TMs bases on Neel's models which only considers doping effect of Ti^{4+}. The master curve considers both Ti^{4+} doping effect and redox reactions [10]. It is used to derive the R for synthesized TMs by calculated lattice parameters. Compared with the R value from models, TM50–80 have higher R while TM90 has lower R. That means $Fe^{3+} \to Fe^{2+}$ happens in TM50 to TM80 and $Fe^{2+} \to Fe^{3+}$ occurs in TM90, which agrees with the redox states.
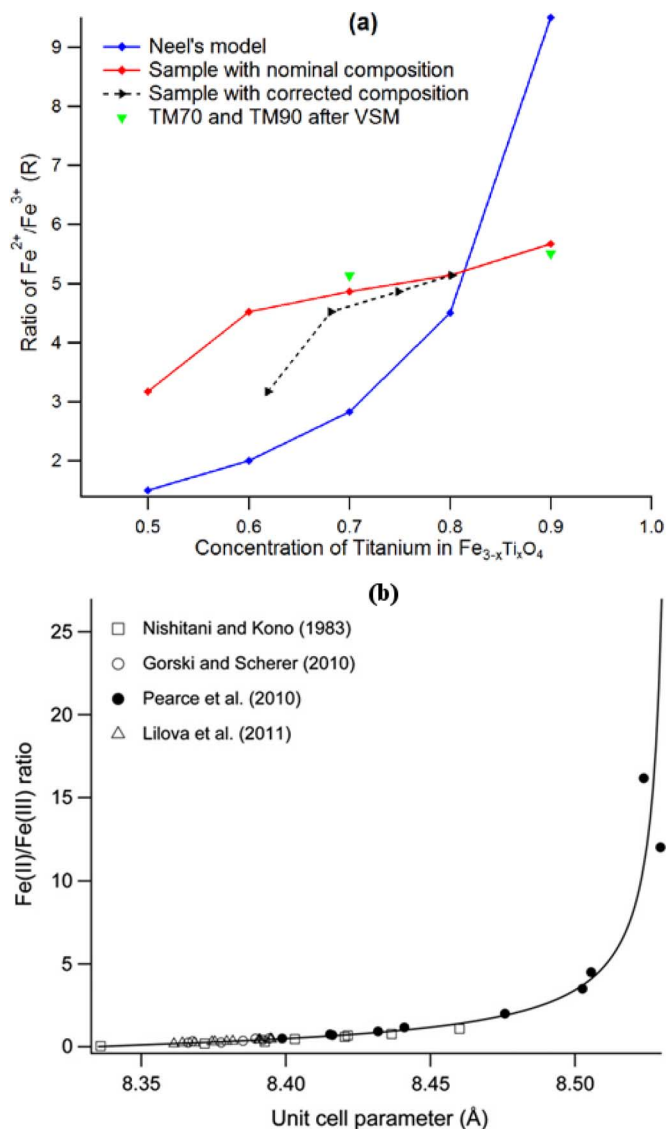

Fig. 4. (a) Fe^{2+}/Fe^{3+} ratio (R) for as-quenched TM samples according to master curve. (b) Master curve Fe(II)/Fe(III) ratio and cell parameter of titanomagnetites [10].

B. Wustite Formation

The secondary wustite phase has an NaCl structure with close paced oxygen. (220) plane of FeO forms first during Fe_3O_4 reduction [11]. Wustite tends to be non-stochiometric ($Fe_{1-x}O$) with clustering of cations and vacancies. The general structure formula of $Fe_{1-x}O$ is

$$\left[Fe^{2+}_{1-3x}Fe^{3+}_{2x-t}\square_{x+t}\right]^{VI}\left[Fe^{3+}_t\right]^{IV}O^{2-}$$
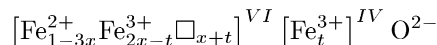
where $0.04 < x < 0.12$ and $2 < (x+t)/t < 4.5$ [12]. Equations (3)–(6) describe the possible formation reaction of wustite in titanomagnetites. Reaction (3) occurs at low $f(O_2)$. The double helix formed by tetrahedral and octahedral interstices in spinel structures [13] can facilitate the diffusion of interstitials. Oxygen interstitials act as a medium to transport electrons to Fe^{3+} ions, as (4) and (5) indicate. Vacancies produced can diffuse to cluster near tetrahedral Fe^{3+} to form non-stoichiometric wustite ($Fe_{1-x}O$) [12]. After electron transfer,
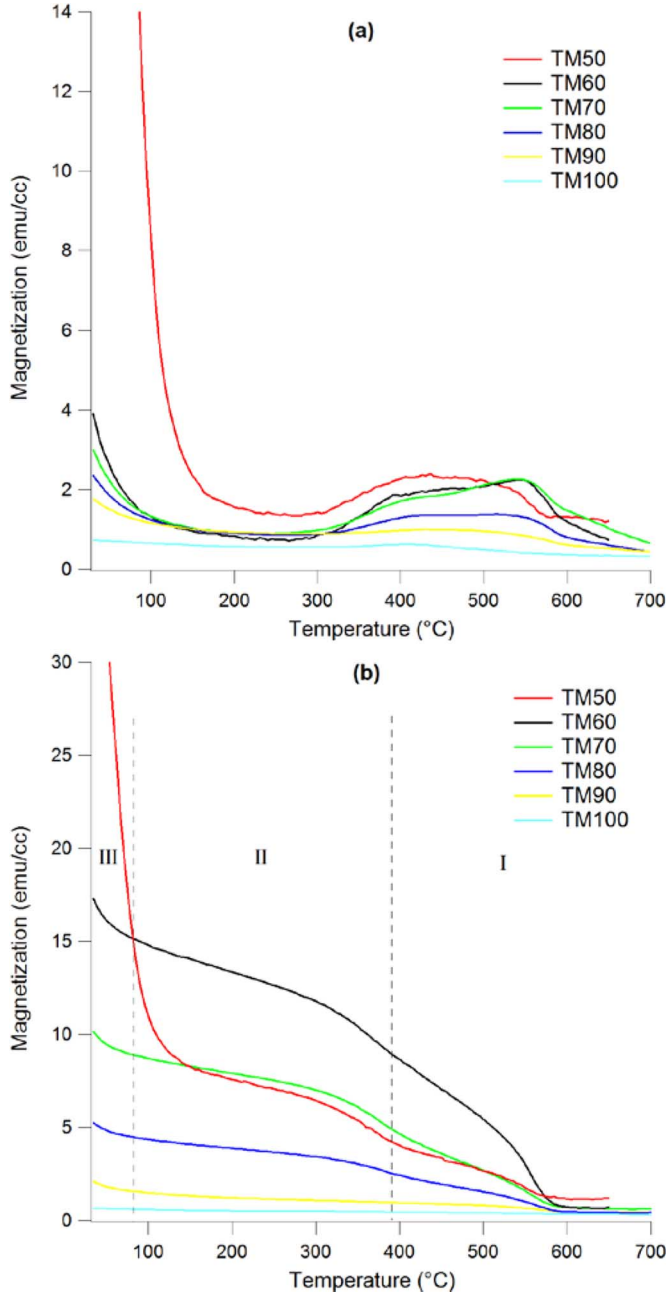
Fig. 5. Magnetization versus temperature of TMs under 0.3 T: (a) heating; (b) cooling.

TABLE II
MULTIPHASE BRILLOUIN FUNCTION FITTING FOR M(T) COOLING CURVE

Sample		T_c (°C)				
		TM50	TM60	TM70	TM80	TM90
Phase I	value	580	570	569	585	635
	phase	Mag	Mag	Mag	Mag	Magh
Phase II	value	384	395	405	403	null
	phase	TMH	TMH	TMH	TMH	null
Phase III	value	72	58	51	53	61
	phase	TM	TM	TM	TM	TMH

Sample		M_s (emu/cc)				
		TM50	TM60	TM70	TM80	TM90
Phase I	value	5.2	11.2	5.6	2.95	1.21
	phase	Mag	Mag	Mag	Mag	Magh
Phase II	value	3.3	3.6	3.23	1.34	null
	phase	TMH	TMH	TMH	TMH	null
Phase III	value	58.2	5.9	3.7	2.5	1.85
	phase	TM	TM	TM	TM	TMH

$P(O_2)$. The oxygen produced inside accumulates in pores and increases $P(O_2)$. The higher $P(O_2)$ blocks reaction (6) and slows wustite formation. A radial $f(O_2)$ gradient from gas-solid surface to the center of solid-solid surface during sintering is proposed. The trend in Fig. 1(b) can also be explained. When the at.% of Fe_2TiO_4 is increased, there is less Fe^{3+} as electron receiver for reaction (4) and (5). Under the same sintering atmosphere, less wustite will form.

C. Temperature Dependent Magnetization

Magnetization, M(T), in spinel ferrites depends on the cation disorder [14], [15]. M(T) on heating in Fig. 5(a) jumps near ~300°C. Ferrimagnetic Fe_3O_4 formed in heating is a phase that increases measured magnetization, which is possibly governed by spinodal decomposition or precipitation. Due to the miscibility gap in this pseudo-binary system, titanomagnetite can separate into magnetite-rich and ulvospinel-rich regions by spinodal decomposition [1]. Magnetite can also precipitate from non-stoichiometric wustite in temperature range of 250°C to 350°C [16]. Formation of magnetite on heating contributes to the observed magnetization hump and the magnetization drops near T_c of magnetite (580°C).

A M(T) cooling curve was fit with a muti-phase Brillouin function [17], [18]. Fitted T_c and M_s for different magnetic phases are summarized in Table II. For TM50–80, temperature ranges denoted I and III correspond to magnetite and titanomagnetite. Given the accuracy of fitting, titanomagnetite phases have similar T_c, indicating similar Ti concentration according to dilution effect of non-magnetic Ti^{4+} on T_c. Another phase in range II is fit with T_c of 400°C. This phase is present in TM50–80 with wustite inside and absent in TM90 and TM100 which are single TM phase. Phase II is postulated to be titanomaghemite formed by Ti^{4+} diffusing to oxidized wustite. For TM90, phase I is maghemite and changes continuous to

oxygen atoms [O] diffuse to the oxygen-deplete surfaces and combine as oxygen molecules:

$$O_o^* \rightarrow O_i'' + V_{\ddot{o}} \qquad (3)$$
$$O_i'' \rightarrow [O] + 2e \qquad (4)$$
$$Fe^{3+} + e \rightarrow Fe^{2+} \qquad (5)$$
$$[O] + [O] \rightarrow O_2. \qquad (6)$$

The distribution of wustite in pellets (Fig. 2) suggests a wustite formation mechanism. The above reactions occur on both gas-solid surfaces of pellets and in pores. Wustite is found primarily near the gas-solid surface because the oxygen formed nearby can be removed by flushing argon maintaining low

phase III, titanomaghemite. During VSM, TM90 is further oxidized, as indicated by smaller Fe^{2+}/Fe^{3+} ratio in Fig. 4(a). Since T_c of maghemite is larger than magnetite, the Ti^{4+} concentration in TM90 is higher than in TM50–80. TM100 is pure antiferromagnetic ulvospinel (T_N-125 K) [19] and the T_N is out of the temperature range of our VSM study.

The wt.% of wustite in TM70 sample after VSM is 0.05%, much less than the initial amount 6.24%. The decrease of wustite amount after VSM runs demonstrates the decomposition and oxidization of wustite in the heating-cooling loop during magnetization measurement. The oxidation of TMs is probably caused by the impure argon and oxygen in VSM sample holder. The Fe^{2+}/Fe^{3+} ratio of samples after VSM decreases due to oxidation. The calculated Fe^{2+}/Fe^{3+} ratio of TM90 after VSM obeys such trend. For TM70 after VSM, the trend is violated, which may be caused by the error in fitting high angle XRD peaks to calculate the lattice parameter.

V. CONCLUSION

Ti-rich titanomagnetite $Fe_{3-x}Ti_xO_4$ synthesized in an oxygen-reducing environment have a significant amount of wustite when $x \leq 0.6$. The amount of this second phase decreases as x increases. Thus, atmospheric conditions are important in samples less than TM50. This may be important in understanding whether spinodal or chemical decomposition occurs. Wustite forms primarily near gas-solid surfaces. The distribution of second phases depends on the oxygen fugacity gradient in sintering. The wustite produces titanomaghemite during its decomposition and oxidation process, which may contribute to magnetic transitions of minerals on Mars.

REFERENCES

[1] A. T. Wise, M. Saenko, A. M. Velázquez, D. E. Laughlin, M. Diaz-Michelena, and M. E. McHenry, "Phase evolution in the Fe_3O_4-Fe_2TiO_4 pseudo-binary system and its implications for remanent magnetization in Martian minerals," *IEEE Trans. Magn.*, vol. 47, pp. 4124–4127, 2011.

[2] V. Raghavan, *Phase Diagrams of Ternary Iron Alloys*.   Metals Park, OH, USA: ASM International, 1987.

[3] T. Owen, K. Biemann, D. R. Rushneck, J. E. Biller, D. W. Howarth, and A. L. Lafleur, "The composition of the atmosphere at the surface of Mars," *J. Geophys. Res.*, vol. 82, pp. 4635–4639, 1977.

[4] E. Park, S. B. Lee, O. Ostrovski, D. J. Min, and C. H. Rhee, "Reduction of the mixture of titanomagnetite ironsand and hematite iron ore fines by carbon monoxide," *ISIJ Int.*, vol. 44, pp. 214–216, 2004.

[5] D. S. Chen, B. Song, L. N. Wang, T. Qi, Y. Wang, and W. J. Wang, "Solid state reduction of panzhihua titanomagnetite concentrates with pulverized coal," *Minerals Eng.*, vol. 24, pp. 864–869, 2011.

[6] R. Sanz, M. Cerdan, A. T. Wise, M. E. McHenry, and M. Diaz-Michelena, "Temperature dependent magnetization and remanent magnetization in pseudo-binary $(Fe_2TiO_4)x$-$(Fe_3O_4)1-x$ $(0.30 < x < 1.00)$ titanomagnetites," *IEEE Trans. Magn.*, vol. 47, pp. 4128–4131, 2011.

[7] M. Sorescu, T. Xu, A. Wise, M. Diaz-Michelena, and M. E. McHenry, "Studies on structural, magnetic and thermal properties of xFe_2TiO_4-$(1-x)Fe_3O_4$ $(0 \leq x \leq 1)$ pseudo-binary system," *J. Magn. Magn. Mater.*, vol. 324, pp. 1453–1462, 2012.

[8] B. D. Cullity and S. R. Stock, *Elements of X-Ray Diffraction*, 3rd ed. Upper Saddle River, NJ, USA: Pearson Education International, 2001.

[9] M. U. Cohen, "Precision lattice constants from X-ray powder photographs," *Rev. Sci. Instrum.*, vol. 68, pp. 68–74, 1935.

[10] C. I. Pearce, O. Qafoku, J. Liu, E. Arenholz, S. M. Heald, R. K. Kukkadapu, C. A. Gorski, C. M. B. Henderson, and K. M. Rosso, "Synthesis and properties of titanomagnetite $(Fe_{3-x}Ti_xO_4)$ nanoparticles: A tunable solid-state Fe(II/III) redox system," *J. Colloid. Interf. Sci.*, vol. 387, pp. 24–38, 2012.

[11] X. M. Guo, Y. Sasaki, Y. Kashiwaya, and K. Ishii, "Microreaction mechanism in reduction of magnetite to wustite," *Metall. Mater. Trans. B*, vol. 35, pp. 517–522, 2004.

[12] R. M. Hazen and R. Jeanloz, "Wustite ($Fe_{1-x}O$): A review of its defect structure and physical properties," *Rev. Geophys. Space GE*, vol. 22, pp. 37–46, 1984.

[13] V. M. Talanov, "Symmetry principles of the formation of ordered phases of crystals," *Glass Phys. Chem.*, vol. 33, pp. 620–635, 2007.

[14] M. A. Willard, Y. Nakamura, D. E. Laughlin, and M. E. McHenry, "Magnetic properties of ordered and disordered spinel-phase ferrimagnets," *J. Amer. Ceram. Soc.*, vol. 82, pp. 3342–3346, 1999.

[15] Y. Nakamura, P. A. Smith, D. E. Laughlin, M. J. De Graef, and M. E. McHenry, "Structure and magnetic properties of quenched $(Mn_xAl_{1-x})_3O_4$ spinels and hausmannites," *IEEE Trans. Magn.*, vol. 31, pp. 4154–4156, 1995.

[16] Y. L. Shaiovich and R. A. Zvinchuk, "Conditions of magnetite precipitation during decomposition of wustite $Fe_{1-x}O$," *Phys. Status Solidi A*, vol. 48, pp. 543–550, 1978.

[17] N. J. Jones, H. Ucar, J. J. Ipus, M. E. McHenry, and D. E. Laughlin, "The effect of distributed exchange parameters on magnetocaloric refrigeration capacity in amorphous and nanocomposite materials," *J. Appl. Phys.*, vol. 111, p. 07A334, 2012.

[18] K. A. Gallagher, M. A. Willard, V. Zabenkin, D. E. Laughlin, and M. E. McHenry, "Distributed exchange interactions and temperature dependent magnetization in amorphous $Fe_{88-x}Co_xZr_7B_4Cu_1$ alloys," *J. Appl. Phys.*, vol. 85, pp. 5130–5132, 1999.

[19] R. S. Carmichael, *Practical Handbook of Physical Properties of Rocks and Minerals*.   Boca Raton, FL, USA: CRC, 1989.